Fabrication of nanofluidic devices utilizing proton beam writing and thermal bonding techniques

L.P. Wang [a,*], P.G. Shao [a], J.A. van Kan [a], K. Ansari [a], A.A. Bettiol [a], X.T. Pan [b], T. Wohland [b], F. Watt [a]

[a] Centre for Ion Beam Applications, Department of Physics, National University of Singapore, 2 Science Drive 3, Singapore 117542, Singapore
[b] Biophysical fluorescence Laboratory, Department of Chemistry, National University of Singapore, 2 Science Drive 3, Singapore 117542, Singapore

Available online 14 February 2007

Abstract

The fabrication of polymer lab-on-a-chip systems for applications in Chemistry and Biology is one of the envisaged niche areas for the Proton Beam Writing (PBW) technique developed at the Centre for Ion Beam Applications (CIBA). Utilizing a highly focused beam of MeV protons, well-defined nanostructures with smooth and straight side walls have been directly written in a 500 nm to 10 μm thick PMMA layer spin coated onto a Kapton substrate. By subsequently thermally bonding the fabricated structures to bulk PMMA and carefully peeling off the Kapton, nanostructures can be attached to bulk PMMA. Finally, by bonding a PMMA sheet to the bottom side of the structure, an integrated PMMA device with enclosed multiple high aspect ratio nanochannels can be realized. Preliminary experiments conducted in order to test this polymeric device indicate good fluidic properties. The nanochannels can be easily filled with dye solution using both pressure and capillary action in the case of hydrophilic solutions.
© 2007 Elsevier B.V. All rights reserved.

PACS: 81.16.Rf; 81.16.Dn; 47.61.Ne

Keywords: Proton beam writing; Nanofabrication; Thermal bonding; Lab-on-a-chip; Nanofluidics

1. Introduction

Micro fluidic devices have gained phenomenal success over a wide range of scientific fields since their introduction [1,2]. The main advantages of such microfluidic systems include high performance, versatility and fast processing [1]. Most conventional microfluidic systems are fabricated on glass or Silicon substrates and several studies have already demonstrated their analytical capabilities [3,4]. However, the fabrication processes for glass and Si devices can be time-consuming and relatively costly. In contrast, polymers offer an attractive alternative to glass and Si as a substrate material due to their biocompatibility, disposability and low cost. Moreover, replication techniques such as soft lithography, contact imprinting and injection molding enable low cost mass production of polymeric microfluidic systems. In addition to being suitable for mass production, polymers are also suitable for rapid prototyping. For rapid prototyping, direct write techniques have the advantage over mass production techniques because masks or masters are not required [3].

Among the several next generation lithography (NGL) methods explored for this purpose, Proton Beam Writing (PBW), a novel technique developed at Centre for Ion Beam Applications (CIBA) [4,5], has attracted considerable attention. Compared with other lithographic techniques such as electron-beam writing, LIGA and UV lithography, PBW is ideally suited to produce micro/nano fluidic structures, because it allows the formation of nanometre-sized, high aspect ratio structures (pillars, channels) with smooth

---

and vertical sidewalls. Utilizing a highly focused beam of MeV protons or H_2^+, well-defined patterns can be directly written in a suitable resist material (e.g. PMMA, SU8 or HSQ) at feature sizes down to 22 nm [6].

The work presented in this paper describes a method for the fabrication of enclosed nanofluidic channels in PMMA by utilizing the PBW and a new thermal bonding technique. The nanochannels were successfully perfused with a dye solution and characterized using confocal microscopy and Fluorescence Correlation Spectroscopy (FCS).

2. Design and fabrication

In order to test the feasibility of prototyping a nanofluidic device using the PBW technique, a structure consisting of multiple parallel nanochannels connected to micron sized inlet and outlet channels was fabricated. The polymer chosen for this study is PMMA because of its high transparency, biocompatibility and the ability to fabricate nanostructures using PBW. A schematic diagram of the structure is illustrated in Fig. 1. The nanofluidic channels were fabricated using a beam of 2 MeV protons focused down to a spot size below 100×100 nm^2, as measured using a resolution standard made by Zhang et al. [7], and magnetically scanned over an area of 200×200 μm^2. The larger micron sized channels were fabricated by combined magnetic and stage scanning. The stage was scanned over a length of 2 mm at a speed of 10 μm/s while the magnetic scan system moved the beam over a width of 10 μm perpendicular to the movement of the stage. The whole structure, shown in Fig. 2, was patterned in a 2 μm thick PMMA layer spin-coated onto a 50 μm thick Kapton film. Although the nanochannel array is slightly misaligned with the inlet and outlet microchannels, they still couple the input to the output channels. A novel thermal bonding technique was developed in order to seal the micro and nanofluidic structures [8]. Two fluid reservoirs were fabricated by drilling through holes into a 3 mm thick PMMA sheet 10×8 mm^2 in size. The nanofluidic structures were
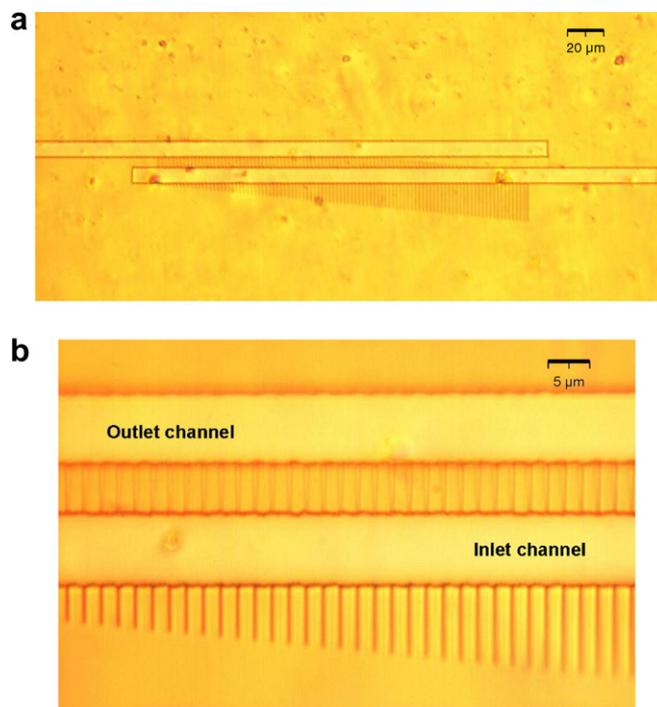

Fig. 2. Optical pictures for proton beam written nanofluidic structure in 2 μm PMMA spin-coated on Kapton film.

thermally bonded to the thick PMMA and then the Kapton substrate was gently peeled off. Fig. 3 shows scanning electron microscope (SEM) images of the nanofluidic channels after bonding to the thick PMMA sheet. The channels are approximately 100 nm in width and 2 μm depth hence the bonding process has not affected the structural integrity of the nanochannels. The quality of the nanochannel side walls (written by PBW) appear good, whereas the much larger inlet and outlet channels have a wavy edge, thought to have been caused by sideways movement of the stage during stage scanning. The final step was to bond a piece of 200 μm thick PMMA sheet to the bottom side of open channels, generating the sandwich-like enclosed PMMA nanofluidic device.
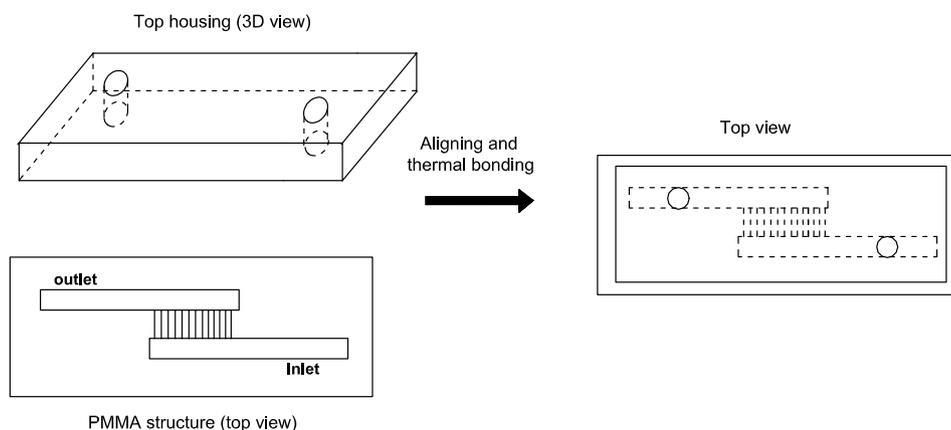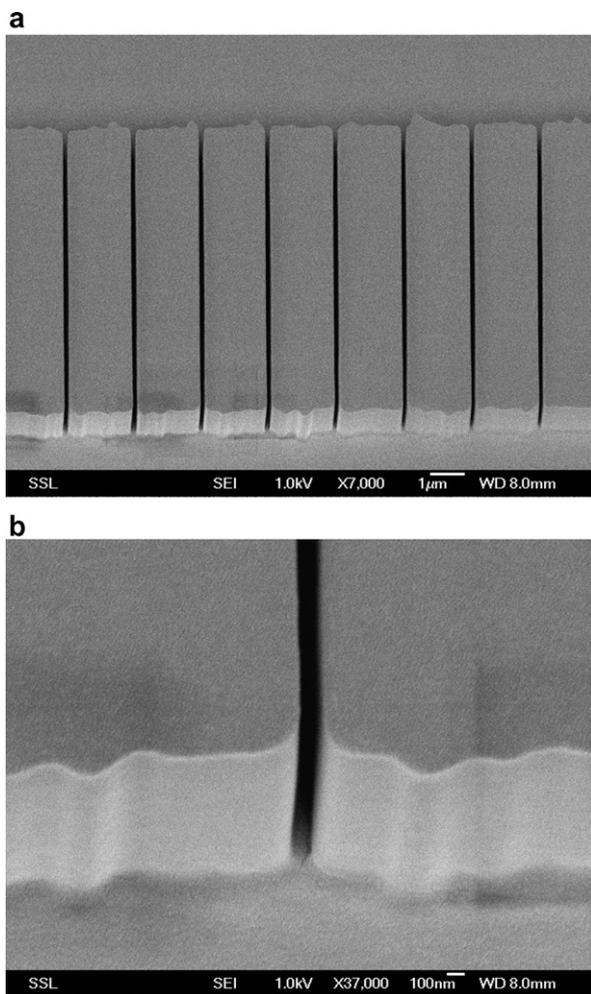

Fig. 1. Nanofluidic structure design and bonding principle.

a

b

Fig. 3. SEM images showing the details of nanochannels transferring to thick PMMA.

3. Device characterization

3.1. FCS setup

There are several publications describing the electro-chemical (e.g. gel electrophoresis; capillary electrophoresis) and electrokinetic performance characteristics of PMMA based microfluidic systems [3,9]. However, there have been very few studies on nanometre-sized polymeric fluidic channels due to the difficulty in making such devices. Fluorescence Correlation Spectroscopy (FCS) was used to test the nanofluidic device due to its high sensitivity and the ability to measure parameters such as diffusion coefficients and the concentration of fluorescent molecules in a fluid [10,11].

The perfusion experiment and FCS measurement were conducted in the Biophysical Fluorescence Laboratory, National University of Singapore. The main optical setup consists of a commercially available laser scanning confocal microscope (FV300, Olympus, Singapore) modified by coupling the emission light out to avalanche photodiodes (SPCM-AQR-14, Pacer Components, UK) for FCS measurements. The generated laser lines (HeNe 543 nm) are directed by an excitation dichroic mirror and scanning mirror to a water immersion objective (60×, NA1.2, Olympus) which focuses the light into fluorescent samples. The fluorescence emission detected from the confocal volume (about 1 femtolitre) is collected by the same objective, introduced through the dichroic mirror, then focused into a small pinhole. The fluorescence at the pinhole is picked up by a lens (Achromats $f = 45$ mm, Linos, Germany), transmitted by an emission filter (595AF60, Omega, USA), finally imaged onto the active area of the APD detector. The TTL output signal from the detector is processed online by an autocorrelator (correlator.com, Zhejiang, China), which produces an experimental autocorrelation curve. Software that
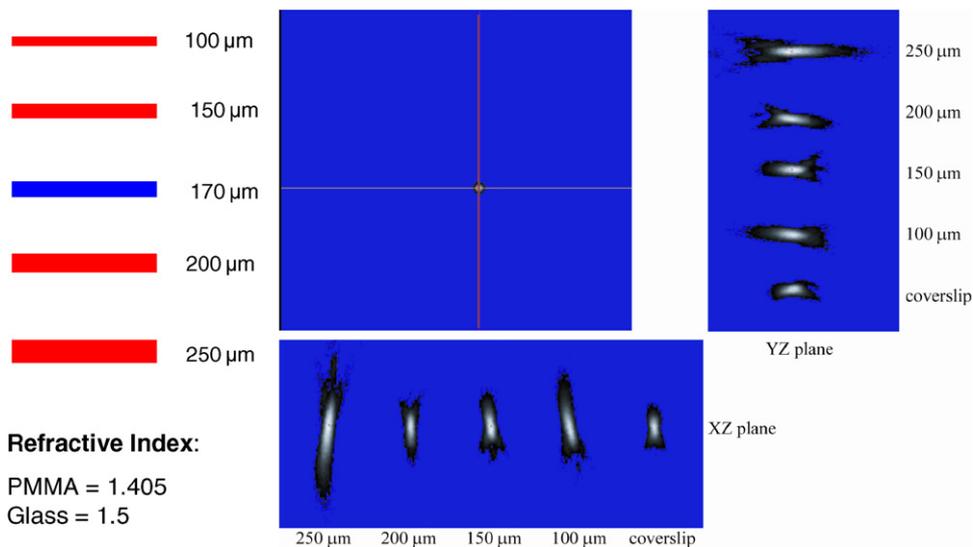

Fig. 4. Optical property characterization of PMMA sheets with different thicknesses (100, 150, 200 and 250 μm respectively) compared with 170 μm glass coverslip.

utilizes a Levenberg–Marquardt algorithm is used to fit the function (program in Igor Pro WaveMatrics, Lake Oswego, OR, USA) in order to extract quantitative results.

In typical FCS experiments, a standard glass coverslip (170 μm) is applied as carrier, through which the focused laser light passes and probes the fluorescent samples. However, the nanofluidic lab-on-a-chip device was fabricated in PMMA. It was therefore necessary to characterize the effect the PMMA has on the point spread function (PSF). Optical property characterization for several substrate material (100, 150, 200, 250 μm PMMA sheet and standard 170 μm glass coverslip) was performed by visualizing transverse projections of the PSF in the X–Y, X–Z and Y–Z plane (see the characterization scheme in Fig. 4). Comparing laser tracks in different observation planes, it was found that 150 or 200 μm PMMA sheet best simulate the use of a conventional glass coverslip.

3.2. Perfusion and fluorescence imaging

To test the effectiveness of the thermal bonded sandwich-like nanofluidic device, a Rhodamine class dye Atto 565 (Sigma, Singapore) at the concentration of 1 nanomolar (nM) was perfused into the channel system by using a syringe pump connecting the two reservoirs. Driven by mechanical force generated by the pump, the fluid navigated through the inlet microchannel (width 8 μm, length 2 mm), successfully passed through the nanochannel (width 100 nm, length 10 μm) array to finally reach the outlet channel.

The complete perfusion was also imaged using the FCS setup. Monitoring of the fluorescence intensity showed that the fluid passed along the inlet channel in around 450 s, and through the nanochannels to the observation area in another 60 s (as shown in Fig. 5). However, the entire diffusion of the fluid into the complete outlet channel took another 4 hours of continuous pumping, which is too time-consuming for a practical device. This time can be shortened by redesigning the chip to reduce the volume of the inlet and outlet channels. Alternatively, since PMMA is naturally hydrophobic [12], a much faster perfusion can be performed by utilizing a syringe to directly inject dye solution containing sodium dodecyl sulphate solution (SDS, 10% in H_2O). SDS is an anionic detergent so it helps to modify PMMA surface to be more hydrophilic thus promoting a rapid capillary action. This will be carried out in the near future.

3.3. FCS measurement in confined nanochannels

The investigation of the confinement effect of nanochannels was carried out by comparing the free diffusion mode of dye Atto 565 in 2 nM concentration in an open volume on standard coverslip, to diffusion in nanochannels. This comparison was investigated using an identical optical setup. Depending on observation positions, a different effective laser probing volume is created [13]. When the
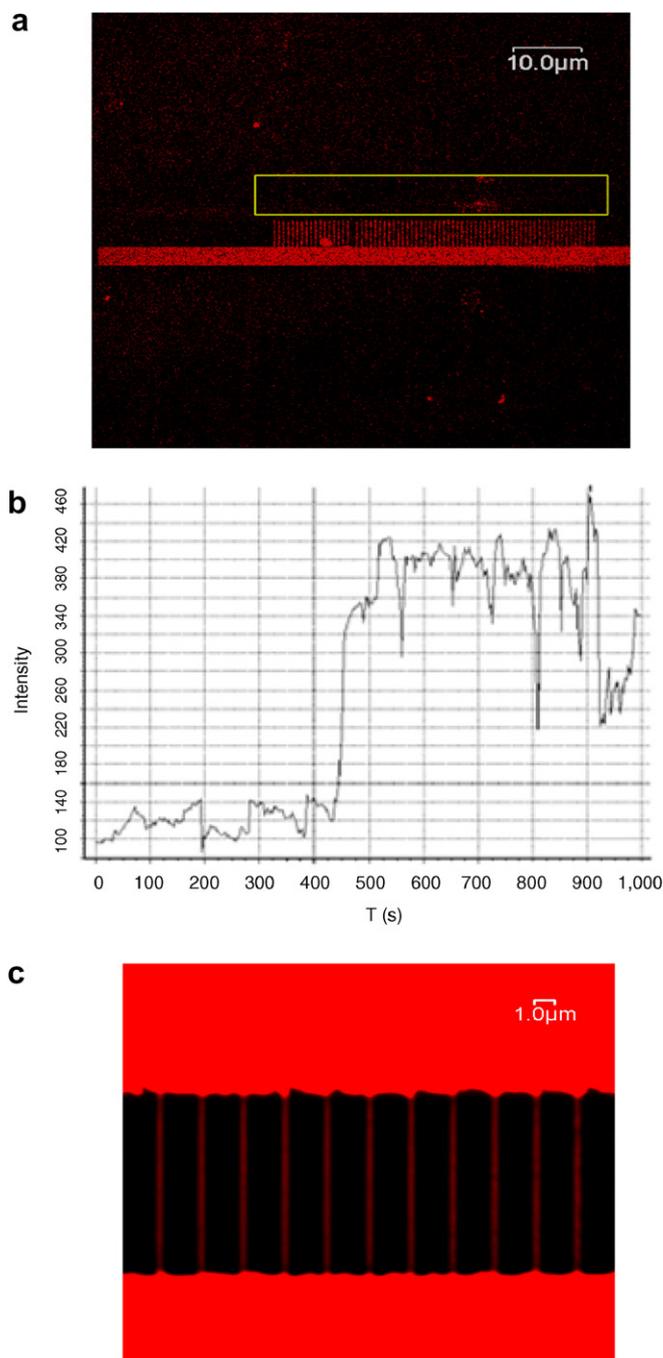

Fig. 5. Fluorescent dye labeled fluidic channels observed using the FCS setup (a) fluid entering the lower inlet microchannel, passing through nanochannels, ready to influx to the outlet microchannel, (b) fluorescence intensity (counts/s) versus time (s) corresponding to the fluorescence monitoring area as given by the rectangle in Fig. 5(a) and (c) Micrograph showing perfused micro/nano fluidic channels.

laser is focused into the fluorescent samples in open volume, there is no confinement in any of the three dimensions. In contrast, when probing into a nanochannel, the laser volume is restricted in one lateral dimension. The fluorescence signals were collected and auto-correlated to generate FCS curves for both experimental conditions. The FCS curve obtained from the open volume was fitted
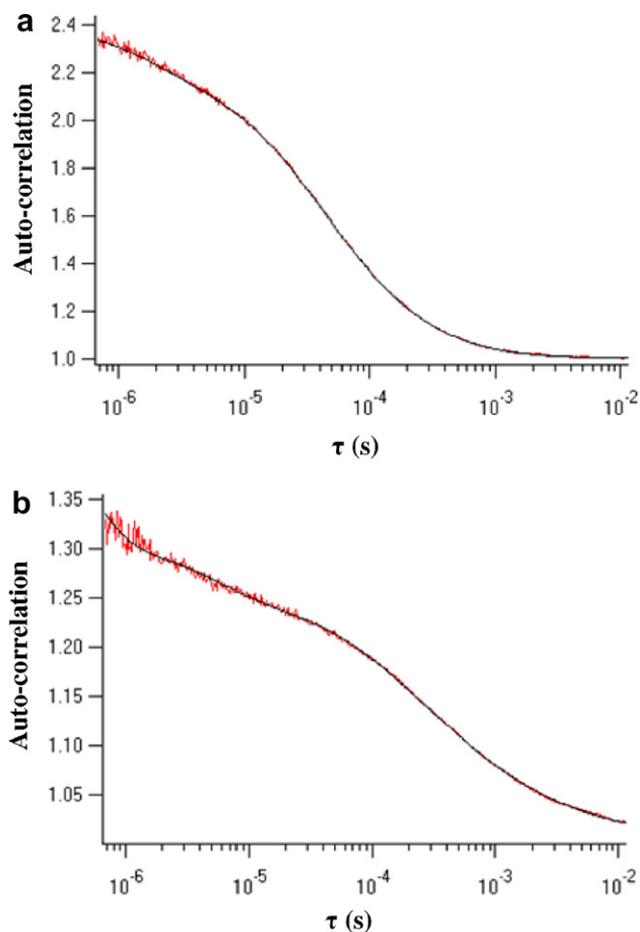
Fig. 6. FCS curves for (a) free diffusion mode and (b) diffusion in confined nanochannel.

with standard three-dimensional Gaussian approximation, while a better fit for confined diffusion case was achieved by using the two-dimensional model. The information contained in the FCS curves in Fig. 6(b) reflects the boundary confinement in the nanochannels, with the long time tail observed in the nanochannel FCS curve (b) corresponding to a longer diffusion time, when compared to (a). This phenomemon will be studied further.

4. Conclusion

The fast prototyping of enclosed nanofluidic devices has been realized through the PBW to accurately pattern nano-size channels in PMMA resist. A new thermal bonding method has been used to seal the polymeric structure into a workable PMMA fluidic chip. The high quality bonding contributes to the good performance of fluidic system: (i) the sealing secures fluidic devices against leakage; (ii) it prevents the fast evaporation of filled fluid, which is vital importance for extremely small volume in nanochannels; (iii) it promotes a real nano-capillary movement with the formation of enclosed pure PMMA channels. Perfusion experiments were performed to test the characteristics of the nanofluidic system. Preliminary FCS results show the potential for this device to be applied in future Single Molecule Detection (SMD) experiments. Future work will concentrate on optimizing the prototyping procedure and improving its fluidic performance. This will be achieved by employing electrokinetic force to drive fluid and a detergent to reduce dye absorption onto the capillary wall.

References

[1] D. Figeys, D. Pinto, Anal. Chem. A 71 (2000) 330.
[2] A. Manz, N. Graber, H.M. Widmer, Sensor Actuat. B 1 (1990) 244.
[3] H. Becker, L.E. Locascio, Talanta 56 (2002) 267.
[4] J.A. van Kan, A.A. Bettiol, F. Watt, Appl. Phys. Lett. 83 (2003) 1629.
[5] J.A. van Kan, A.A. Bettiol, B.S. Wee, T.C. Sum, S.M. Tang, F. Watt, Sensor Actuat. A 92 (2001) 370.
[6] J.A. van Kan, A.A. Bettiol, F. Watt, Nano Letters 6 (2006) 579.
[7] F. Zhang, J.A. van Kan, S.Y. Chiam, F. Watt, Nucl. Instr. and Meth. B, these Proceedings, doi:10.1016/j.nimb.2007.02.065.
[8] P.E. Shao, J.A. van Kan, L.P. Wang, K. Ansari, A.A. Bettiol, F. Watt, Appl. Phys. Lett. 88 (2006) 093,515.
[9] K.A. Mahabadi, I. Rodriguez, S.C. Haur, J.A. van Kan, A.A. Bettiol, F. Watt, J. MicroMech. MicroEng. 16 (2006) 1070.
[10] P. Schwille, E. Haustein, <www.bem.uchile.cl/Estructural/Recursos/TeoriaFCS.pdf>.
[11] O. Krichevsky, G. Bonnet, Rep. Prog. Phys. 65 (2002) 251.
[12] H. Bayer, H. Engelhardt, J. Microcol. Sep. 8 (1996) 479.
[13] M. Foquet, J. Korlach, W.R. Zipfel, W.W. Webb, H.G. Craighead, Anal. Chem. 76 (2004) 1618.